



Selective photosensitizer delivery into plasma membrane for effective photodynamic therapy



Jiyoung Kim^{a,b,1}, Olavo Amorim Santos^{a,b,1,2}, Ji-Ho Park^{a,b,c,*}

^a Department of Bio and Brain Engineering, Korea Advanced Institute of Science and Technology (KAIST), 291 Daehak-ro, Yuseong-gu, Daejeon 305-701, Republic of Korea

^b KAIST Institute for Optical Science and Technology, KAIST, 291 Daehak-ro, Yuseong-gu, Daejeon 305-701, Republic of Korea

^c KAIST Institute for the NanoCentury, KAIST, 291 Daehak-ro, Yuseong-gu, Daejeon 305-701, Republic of Korea

ARTICLE INFO

Article history:

Received 1 April 2014

Accepted 24 May 2014

Available online 2 June 2014

Keywords:

Cancer
Drug delivery
Membrane fusogenic liposome
Photodynamic therapy
Photosensitizer

ABSTRACT

Subcellular localization of photosensitizers (PSs) determines the therapeutic efficacy in the photodynamic therapy. However, among the subcellular compartments, there has been little effort to deliver the PSs selectively into the plasma membrane and examine the phototherapeutic efficacy of membrane-localized PSs. Here, we developed a liposomal delivery system to localize the hydrophobic PSs selectively into the plasma membrane. The membrane fusogenic liposomes (MFLs), the membrane of which is engineered to fuse with the plasma membrane, was prepared for the membrane localization of PSs. The phototherapeutic efficacy of cells treated with ZnPc-loaded MFLs was superior over that of cells treated with ZnPc-loaded non-fusogenic liposomes, which is the conventional liposomal formulation that delivers the PSs into the intracellular compartments *via* endocytosis. The membrane localization of ZnPc molecules led to rapid membrane disruption upon irradiation and subsequent necrosis-like cell death. The membrane-localized generation of reactive oxygen species in the cells treated with ZnPc-loaded MFLs was likely to account for the effective disruption of plasma membrane. Thus, this work provides a novel delivery method to localize the PSs selectively into the plasma membrane with the enhanced phototherapeutic efficacy.

© 2014 Elsevier B.V. All rights reserved.

1. Introduction

In the past decades, the adjuvant cancer treatment has evolved from conventional radiotherapy and chemotherapy to new approaches that diminish tumor growth [1]. In this scenario, photodynamic therapy (PDT) emerged as an efficient alternative, presenting potential advantages when compared to the conventional methods [2,3]. This non-surgical and minimally invasive treatment has been clinically approved and has been used for the management of different neoplastic pathologies [4,5], such as lung, head and neck, and brain cancer. The PDT is also considered to be the ideal treatment for skin cancer [6].

The mechanism of action of PDT consists in the uptake of a photosensitizer (PS) by the diseased setting, followed by irradiation with a specific wavelength of light, which activates the PSs and promotes cell death [3,7]. Once irradiated, the PS is transformed into an excited state, transferring energy to its surrounding molecular oxygen and

generating reactive oxygen species (ROS), primarily singlet oxygen. Due to its short half-life, the singlet oxygen diffuses up to tens of nanometer and, therefore, the damage produced is limited to the subcellular location of the PS. The subcellular localization sites of PSs include plasma membrane, lysosome, Golgi apparatus, nucleus, and mitochondrion [8,9]. The chemical natures of PSs, including size, charge, amphiphilicity, and partition coefficients, are important parameters that influence the subcellular localization. Furthermore, it was shown that the subcellular localization of PSs determined the therapeutic efficacy in the PDT [10–14]. Thus, the subcellular location of PSs delivered to the cells during the irradiation period becomes an important variable and can lead to enhancement of therapeutic outcome in the PDT. However, most of PSs are insoluble or easily aggregated in physiological conditions due to their hydrophobicity, restricting the selective delivery to target cells and subsequent subcellular compartments.

Several approaches have been proposed to overcome such limitations, including the use of nanocarriers to encapsulate and deliver the PSs selectively to the intracellular sites [15–23]. Amongst them, liposomes have been broadly studied as PS nanocarriers in the past few years because of their biocompatibility and stable PS entrapment [24–26]. Particularly, liposomes allow for efficient loading of hydrophobic PSs into their transmembranes [27,28]. Furthermore, liposomes can be designed to interact with cells differently by engineering their lipid composition. The interactions can occur through two major processes, such as endocytosis and fusion [29]. Conventional liposome formulations developed

* Corresponding author at: Department of Bio and Brain Engineering, KAIST Institute for Optical Science and Technology, and KAIST Institute for the NanoCentury, Korea Advanced Institute of Science and Technology (KAIST), 291 Daehak-ro, Yuseong-gu, Daejeon 305-701, Republic of Korea.

E-mail address: jihopark@kaist.ac.kr (J.-H. Park).

¹ J.K. and O.A.S. contributed equally to this work.

² Present address: Department of Physics, Universidade Federal de São Carlos, São Carlos, Brazil.

for intracellular drug delivery, including cationic and ligand-conjugated ones, typically enter the cell *via* endocytosis. The PSs delivered into the cell by such liposomes are mainly localized in the intracellular compartments, such as mitochondrion, Golgi apparatus, lysosome and nucleus. However, there has been little effort to localize the PSs selectively into the plasma membrane although the damage to this structure is also known as a major contributing factor to the overall PDT outcome [30–33].

In this work, we developed a liposomal delivery system to localize the PSs selectively into the plasma membrane and examined the therapeutic efficacy of PSs localized in the membrane compared to that of PSs delivered to the cytoplasm by conventional liposomes (Fig. 1). Zinc phthalocyanine (ZnPc) was used as a PS because of its lipophilicity to allow the membrane localization and strong phototoxicity upon NIR irradiation [10,17,19,28,34]. The ZnPc molecules were delivered selectively into the plasma membrane by membrane fusogenic liposomes (MFLs), the membrane of which is designed to fuse with the plasma membrane [35]. Conventional cationic liposomes (referred here as non-fusogenic liposomes, NFLs), which enter the cells *via* endocytosis, were also used to deliver the ZnPc molecules into the intracellular compartments, primarily endosome/lysosome. The phototoxicity depending on the subcellular localization of ZnPc molecules was evaluated using MTT assay. Membrane disruption, cellular and nuclear morphological change, and intracellular ROS generation were assessed to determine the mechanism of cellular phototoxicity enhanced by the selective delivery of ZnPc molecules into the plasma membrane.

2. Materials and methods

2.1. Cell lines

Murine colon carcinoma CT26 cells and human non-small cell lung cancer H460 cells were cultured in RPMI 1640 medium (Hyclone), with added 10% fetal bovine serum (FBS, Hyclone) and 10 mL of antibiotics (penicillin 100 units/mL + streptomycin 100 µg/mL, Hyclone).

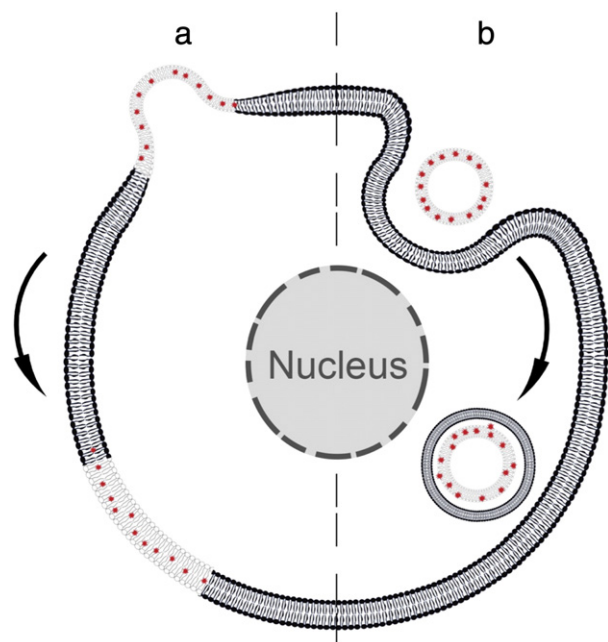


Fig. 1. Schematic of selective subcellular delivery of hydrophobic photosensitizers by synthetic liposomes. (a) Membrane fusogenic liposomes (MFLs), the membrane of which is designed to fuse with the plasma membrane, deliver the photosensitizers (red) selectively into the plasma membrane. (b) Conventional cationic liposomes (referred here as non-fusogenic liposomes, NFLs), which enter the cell *via* endocytosis, deliver the photosensitizers into the intracellular compartments.

Human brain glioblastoma U-87 MG cells were cultured in DMEM medium (Hyclone) with added 10% FBS and 10 mL antibiotics. The cells were maintained incubated at 37 °C in a 5% CO₂-containing atmosphere.

2.2. Preparation and characterization of ZnPc-loaded liposomes

ZnPc-loaded MFLs and NFLs were prepared from 1,2-dimyristoyl-sn-glycero-3-phosphocholine (DMPC, Avanti Polar Lipids), 1,2-distearoyl-sn-glycero-3-phosphoethanolamine-N-[methoxy(polyethylene glycol)-2000] (DSPE-PEG, Avanti Polar Lipids), 1,2-dioleoyl-3-trimethylammonium-propane (DOTAP, Avanti Polar Lipids), and ZnPc (Sigma) at the molar ratio of 74.5:3.8:20:1.7 and 78.3:0:20:1.7 by film hydration/extrusion method, respectively, purified with a centrifugal filter (Amicon® Ultra-4 100K, Millipore), and stored in PBS at 4 °C before use. The hydrodynamic size and zeta potential of liposomes were measured using dynamic light scattering (Zetasizer Nano ZS90, Malvern Instruments). The absorbance and fluorescence of ZnPc-loaded liposomes were measured using UV–vis spectrophotometer (SpectraMax Plus384, Molecular Devices) and spectrofluorometer ($\lambda_{\text{ex}} = 600$ nm and $\lambda_{\text{em}} = 680$ nm in the fluorescence measurements, Gemini XPS, Molecular Devices), respectively. In order to test loading stability of ZnPc in the liposomes in the physiological condition, ZnPc-loaded liposomes were incubated in PBS containing 10% serum for 2 h at 37 °C and washed with the centrifugal filter to remove free ZnPc released from the liposomes. The absorption spectra of ZnPc-loaded liposomes at pre-incubation and 2 h post-incubation were obtained using UV–vis spectrophotometer.

2.3. Cellular uptake of ZnPc-loaded liposomes

Three kinds of cancer cells (H460 human non-small cell lung cancer, CT26 mouse colon carcinoma, and U87MG human glioblastoma) were treated with ZnPc-loaded liposomes or free ZnPc molecules at ZnPc concentrations of 5.192, 9.344 or 15.575 µM for 30 min and washed with fresh medium. To visualize subcellular localization of ZnPc delivered by liposomes, the ZnPc-treated cells were stained with Hoechst 33342 (Invitrogen), and imaged using a confocal fluorescence microscope (Nikon). To quantify the intracellular amount of ZnPc delivered by liposomes, the ZnPc-treated cells were incubated with 200 µL of RIPA buffer (Sigma) for 30 min to solubilize the cellular lipid and proteins. The ZnPc fluorescence of cell lysate was measured using a spectrofluorometer ($\lambda_{\text{ex}} = 600$ nm and $\lambda_{\text{em}} = 680$ nm in the fluorescence measurements).

2.4. In vitro photodynamic therapy

Three kinds of cancer cells (H460, CT26, and U87MG) were treated with ZnPc-loaded liposomes at various ZnPc concentrations (0 µM, 0.363 µM, 1.417 µM, 5.192 µM and 15.575 µM) for 30 min and washed with fresh medium. The cells were irradiated with a 660 nm laser (10 J) and further incubated for 24 h. The cell viability was evaluated using a 3-(4,5-dimethylthiazol-2-yl)-2,5-diphenyltetrazolium bromide (MTT) assay (Invitrogen). In order to test effects of time-dependent intracellular migration of ZnPc localized in the plasma membrane on the PDT, the cells were treated with ZnPc-loaded liposomes for 30 min, washed, and further incubated for 2 or 4 h prior to the laser irradiation (10 J).

The cell death in the early stages after PDT was also examined using calcein-AM assay (Invitrogen). The culture medium containing the calcein-AM was prepared by dissolving the calcein-AM in the culture medium without phenol red (1.25 µg/mL). The H460 cells were treated with ZnPc-loaded liposomes at a ZnPc concentration of 5.192 µM for 30 min and washed with fresh medium. After irradiation (660 nm, 10 J), the cells were immediately incubated in the medium containing the calcein-AM for 30 min, washed, and treated with 200 µL of RIPA buffer (Sigma). The Calcein fluorescence was then measured using a spectrofluorometer ($\lambda_{\text{ex}} = 490$ nm and $\lambda_{\text{em}} = 515$ nm).

2.5. Cellular and nuclear morphology imaging

In the following experiments, we adjusted the concentrations of liposomes added to the H460 cells in order to deliver the similar amount of ZnPc molecules to the H460 cells over the treatment period. To observe cellular morphological change induced by PDT, GFP-expressing H460 cells were treated with ZnPc-loaded MFLs at a ZnPc concentration of 5.192 μM or with ZnPc-loaded NFLs at a ZnPc concentration of 3.635 μM for 30 min and washed with fresh medium. Immediately or 4 h after irradiation (660 nm, 3.3 or 10 J), the cells were imaged using a confocal fluorescence microscope. To observe nuclear morphological change induced by PDT, H460 cells were treated with ZnPc-loaded liposomes for 30 min and washed with fresh medium. After irradiation (660 nm, 10 J), the cells were immediately stained with ethidium homodimer-1 (EthD-1, 4 μM , Invitrogen) or Hoechst 33342 (0.5 mg/mL, Sigma) and imaged using a confocal fluorescence microscopy.

2.6. Intracellular ROS imaging and assay

H460 cells were pre-loaded with 2,7-dichlorodihydrofluorescein diacetate (DCFH-DA, Cell Biolabs, Inc.) for 45 min and washed with fresh medium. The cells were then treated with ZnPc-loaded MFLs at a ZnPc concentration of 5.192 μM or ZnPc-loaded NFLs at a ZnPc concentration of 3.635 μM for 30 min, washed with fresh medium, and irradiated with a 660 nm laser (10 J). For intracellular ROS imaging, the DCF fluorescence in the cells was imaged using a confocal fluorescence microscope immediately after irradiation. For intracellular ROS assay, the cells were incubated for 30 min after irradiation and then lysed with a lysis buffer (2 \times , Cell Biolabs, Inc.) and the DCF fluorescence of cell lysate was measured using a spectrofluorometer ($\lambda_{\text{ex}} = 480 \text{ nm}$ and $\lambda_{\text{em}} = 530 \text{ nm}$). The DCF fluorescence in each sample was normalized to the untreated sample.

2.7. Statistics

Statistical analyses of the data were performed using *t* test and ANOVA. All experiments were performed at least three times.

3. Results and discussion

ZnPc-loaded MFLs were prepared to deliver the ZnPc molecules selectively into the plasma membrane using a previously established protocol with some slight modifications [35]. ZnPc-loaded NFLs were also prepared as a conventional cationic liposomal formulation to deliver the ZnPc molecules into the intracellular compartments *via* endocytosis. The hydrodynamic sizes of ZnPc-loaded liposomes appeared in the range of 119–124 nm ($119.8 \pm 11.57 \text{ nm}$ for MFLs and $123.7 \pm 6.07 \text{ nm}$ for NFLs). The surface charges of ZnPc-loaded liposomes, which determined their cellular uptake patterns, exhibited the difference because of their lipid compositions ($22.0 \pm 1.7 \text{ mV}$ for MFLs and 53.3 ± 1.9 for NFLs). The absorbance and fluorescence measurements of both ZnPc-loaded liposomes revealed accentuated peaks at 670 nm and 680 nm, respectively, which is in accordance with the typical absorbance and fluorescence spectra of ZnPc molecules [34]. The ZnPc incorporated into the liposomal membrane was not significantly released in the biological medium over an incubation period of 2 h, indicating good stability of the incorporated ZnPc (Supplementary Fig. S2).

We first observed the subcellular localization of ZnPc molecules delivered by synthetic liposomes in three kinds of cancer cell lines (H460 human non-small cell lung cancer, CT26 mouse colon carcinoma, and U87MG human glioblastoma). The cells were treated with ZnPc-loaded liposomes or free ZnPc molecules at a ZnPc concentration of 9.344 μM for 30 min, washed, and imaged using confocal fluorescence microscopy. Intrinsic fluorescence of ZnPc molecules allowed visualization of their subcellular localization. As expected, MFLs delivered the

ZnPc molecules primarily into the plasma membranes of cancer cells over a 30-min treatment period (Fig. 2a). On the other hand, the ZnPc molecules delivered intracellularly by NFLs were observed as dots in the cytoplasm, indicating that most of ZnPc molecules were trapped in the endosomes/lysosomes alongside the NFLs. Additionally, the cells treated with free ZnPc molecules showed that relatively smaller amounts of ZnPc were translocated into the cells and most of them were observed in the perinuclear region (Supplementary Fig. S3). To determine the intracellular amount of ZnPc molecules delivered by synthetic liposomes, the cells were lysed to solubilize the cellular lipids and proteins after liposome treatment. The ZnPc fluorescence of cell lysate was measured using a spectrofluorometer. Highly cationic NFLs delivered considerably larger quantities of ZnPc molecules into the intracellular region, compared to the MFLs (2.13-, 3.27-, and 3.54-fold uptake in H460, CT26 and U87MG cells, respectively, Fig. 2b). As

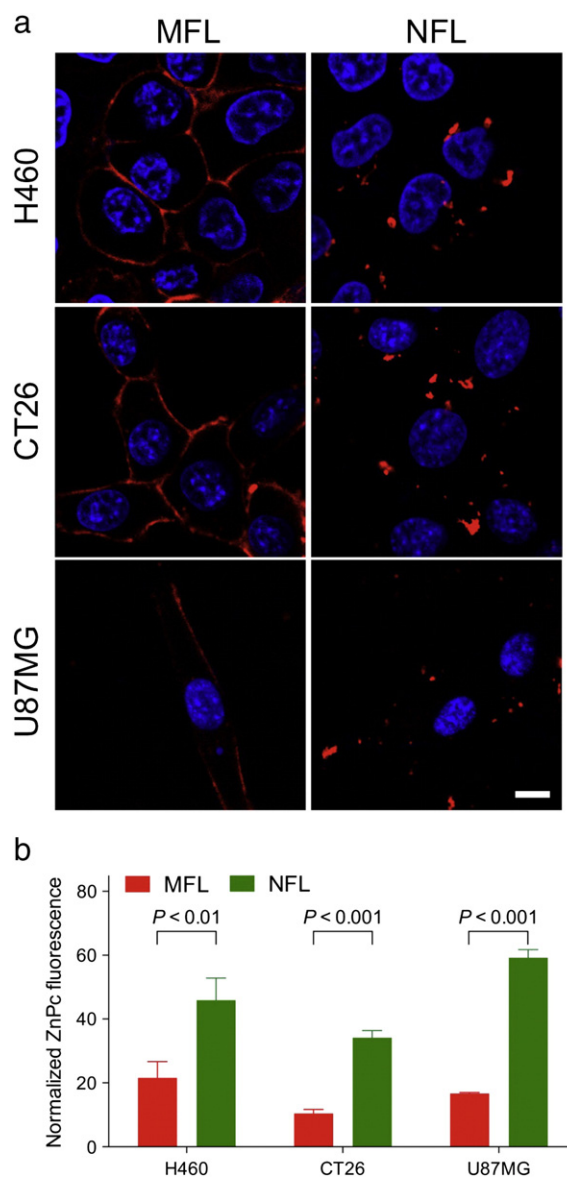


Fig. 2. Selective subcellular delivery of ZnPc molecules by synthetic liposomes. (a) Confocal microscopic images of cancer cells (H460, CT26, and U87MG) treated with synthetic liposomes loaded with hydrophobic ZnPc (red) for 30 min. Nuclei were stained with Hoechst 33342 (blue). Scale bar indicates 2 μm . (b) Quantification of ZnPc fluorescence in the cells treated with ZnPc-loaded liposomes. The cells were lysed to solubilize the cellular lipid and proteins after liposome treatment. The ZnPc fluorescence of cell lysate was measured using a spectrofluorometer and normalized to the cell number ($n = 4$; error bars = s.d.; $P < 0.01$, $P < 0.001$ by unpaired *t* test).

observed in the previous studies [36,37], the surface charge of liposomes strongly influences the cellular uptake, which typically increases with cationic ones. Furthermore, while the intracellular amount of ZnPc delivered by NFLs was increased proportionally with the liposome (ZnPc) concentration at which the cells were treated, the amount of ZnPc localized in the membrane by MFLs was not increased above the concentration of 9.344 μM ZnPc (Supplementary Fig. S4). It can be reasoned that the space in the plasma membrane that can be occupied with ZnPc molecules seems to be restricted, unlike the cytoplasm. The membrane-specific delivery was independent of the MFL (ZnPc) concentration treated (Supplementary Fig. S5). Collectively, these results demonstrate that MFLs enable efficient and selective delivery of hydrophobic PSs into the plasma membrane of cancer cells although they deliver relatively small amounts of PSs to the cells.

Next, we assessed the phototherapeutic efficacy of ZnPc molecules delivered into distinct subcellular compartments (plasma membrane vs. endosome/lysosome). Three kinds of cancer cells (H460, CT26, and U87MG) were treated with ZnPc-loaded liposomes at various ZnPc concentrations for 30 min and washed. Half of the samples were exposed to 660 nm laser irradiation and incubated for additional 24 h, whereas the other was not irradiated. The cell viability was then analyzed using MTT assay. For all three kinds of cells, both samples treated with ZnPc-loaded liposomes showed significant signs of cellular phototoxicity at the ZnPc concentration higher than 1.417 μM (Fig. 3). The phototoxicity increased proportionally with the ZnPc concentration at which the cells were treated. Importantly, the cells treated with ZnPc-loaded MFLs exhibited substantially higher phototoxicity in the ZnPc concentration range of 1.417–15.575 μM , compared to those treated with ZnPc-loaded NFLs. Particularly, the membrane localization of ZnPc molecules in the H460 cells induced more dramatic cell death after irradiation, presumably due to their relatively high sensitivity to PDT [38]. The cells that received laser irradiation alone displayed insignificant phototoxicity, suggesting that the irradiation condition used in this study was biosafe. The liposome treatments at all ZnPc concentrations also did not induce any significant cytotoxicity (Supplementary Fig. S6). These experiments revealed that the selective delivery of ZnPc molecules into the plasma membrane significantly enhanced the therapeutic efficacy of PDT. It should be noted that the intracellular amount of ZnPc molecules in the MFL-treated cells was approximately 2–3.5 times lower than that in the NFL-treated cells (Fig. 2b).

After observing superior phototherapeutic activity of membrane-localized ZnPc molecules, we started to investigate the mechanism behind the cell death. The H460 cell line was particularly chosen as they revealed the highest phototoxicity when the ZnPc molecules were localized in the plasma membrane, compared to other two cell lines (Fig. 3). We first examined the cellular response in the early stages after PDT because it would be responsible for the subsequent cell death. The H460 cells were treated with ZnPc-loaded liposomes for 30 min, washed, and exposed to the laser irradiation. Immediate phototoxic responses of the cells were evaluated using calcein-AM assay. The ZnPc molecules localized in the plasma membrane led to more efficient cell death compared to those localized in the cytoplasm (Fig. 4). We also investigated the effect of intracellular migration of ZnPc molecules localized in the plasma membrane on the phototherapeutic efficacy in the H460 cells because some of hydrophobic ZnPc molecules delivered to the plasma membrane were likely to be internalized to the cytoplasmic membranes or compartments over the incubation period of time (Supplementary Fig. S7a). The phototoxicity of MFL-treated cells was slightly reduced with increasing the incubation time, whereas that of NFL-treated cells was not changed (Supplementary Fig. S7b). However, the phototoxicity of MFL-treated cells at 4 h post-treatment was still significantly higher than that of NFL-treated cells. It indicated that the ZnPc molecules delivered selectively into the plasma membrane retained their superiority in the photodynamic efficacy despite the dynamic intracellular migration. Collectively, these results suggest that the initial phototoxicity mechanism of ZnPc molecules localized in the plasma membrane is somewhat

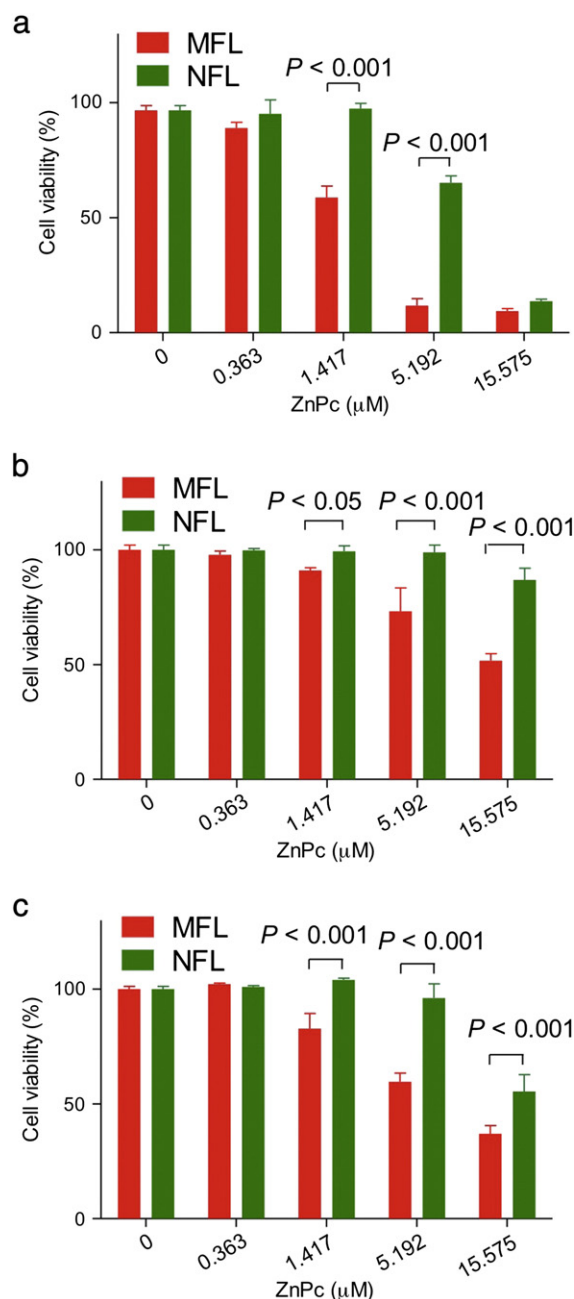


Fig. 3. *In vitro* photodynamic therapy of cancer cells treated with ZnPc-loaded synthetic liposomes. (a–c) Phototoxicity of (a) H460, (b) CT26, and (c) U87MG cells treated with ZnPc-loaded liposomes at various ZnPc concentrations. The cells were treated with ZnPc-loaded liposomes for 30 min, washed, and irradiated with a 660 nm laser. After 24 h incubation, cell viability was analyzed by MTT assay ($n = 3–4$; error bars = s.d.; $P < 0.05$, $P < 0.001$ by two-way ANOVA).

different from that of ZnPc molecules localized in the intracellular compartments, thereby leading to substantial cell death during and after irradiation.

To understand the mechanism of immediate phototoxic responses of the cells, we also observed the morphological change of cells in the early stages after PDT (Fig. 5). In following experiments, we adjusted the concentrations of liposomes added to the cells in order to deliver the similar amount of ZnPc molecules to the cells over the treatment period because each liposomal formulation showed different delivery efficiency of ZnPc molecules (Fig. 2b). The cells were treated with ZnPc-loaded liposomes for 30 min, washed, and exposed to the laser

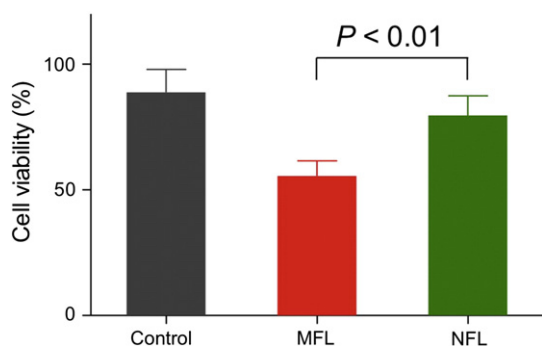


Fig. 4. Initial phototoxicity of H460 cells treated with ZnPc-loaded liposomes. The cells were treated with ZnPc-loaded liposomes for 30 min and irradiated with a 660 nm laser. After irradiation, cell viability was immediately analyzed by calcein-AM assay ($n = 3-4$; error bars = s.d.; $P < 0.01$ by one-way ANOVA). Control indicates the sample irradiated alone.

irradiation for different period of time (1 or 3 min). After irradiation, the GFP fluorescence in the cytoplasm was immediately imaged using a confocal microscope. After 1 min irradiation, multiple protuberances of the plasma membrane was observed in the cells treated with MFLs, whereas the cells treated with NFLs did not show any distinct morphological change. After 3 min irradiation, the MFL-treated cells lost their original phenotype, which was seen in the cells irradiated alone (control), and appeared considerably rounded. Additionally, the cellular morphology of MFL-treated cells at 4 h post-irradiation appeared substantial cytoplasmic swelling, whereas some of NFL-treated cells displayed the phenotype similar to the cells irradiated alone (Supplementary Fig. 8).

We further assessed the membrane integrity and nuclear morphology of cells exposed to laser irradiation after liposome treatments in order to study the early feature of cell death. The ethidium homodimer-1 (EthD-1), which is a membrane-impermeable fluorescent dye to bind to nucleic acids, was used to simultaneously examine the membrane disruption and nuclear morphological change. After irradiation, the cells were immediately stained with EthD-1 and imaged using a fluorescence microscope. Strong EthD-1 fluorescence was observed in the nuclei of both samples, indicating the membrane disruption (Fig. 6a). However, the nuclear phenotype manifested by MFL-treated cells appeared clearly distinct from that of NFL-treated cells. The peripheral condensed nuclear morphology was observed in most of MFL-treated cells, whereas the NFL-treated cells exhibited the typical condensed morphology and reduced size of nuclei, indicating the apoptotic cell death [10,39,40]. Additionally, the cell stained with Hoechst 33342 immediately after PDT also showed similar nuclear morphological patterns (Fig. 6b), further confirming the EthD-1 staining results. Collectively, these results imply that the selective disruption of plasma membrane loaded with ZnPc molecules upon irradiation may induce necrosis-like cell death, evidenced by peripheral chromatin condensation, cytoplasmic swelling, and plasma membrane disruption [30]. Thus, the membrane disruption-mediated PDT could be further utilized to destroy the apoptosis-resistant cancer cells.

Lastly, we investigated whether the reactive oxygen species (ROS) generated by the ZnPc molecules localized in the plasma membrane accounted for effective membrane disruption and subsequent necrosis-like cell death. The H460 cells preloaded with DCFH-DA, an intracellular ROS fluorescent sensor, were treated with ZnPc-loaded liposomes for 30 min, washed, and irradiated with a 660 nm laser. For intracellular ROS imaging, the cells were imaged using a confocal fluorescence microscope immediately after irradiation. For DCF fluorescence measurements, the cells were lysed after irradiation and the DCF fluorescence of the cell lysate was measured using a spectrofluorometer. The DCF fluorescence, indicating the ROS generation, was clearly observed in both samples treated with synthetic liposomes followed by irradiation, compared to the sample irradiated alone (Fig. 7a). Importantly, the DCF fluorescence

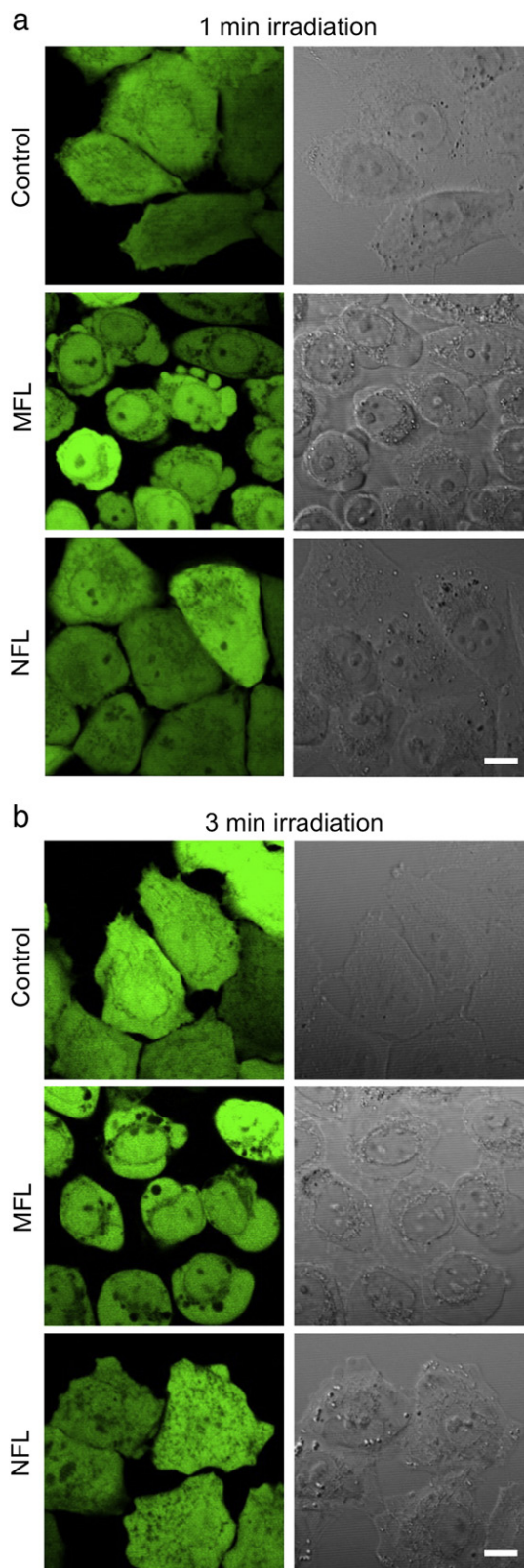


Fig. 5. Morphological changes of H460 cells in the early stages after photodynamic therapy. (a and b) Confocal microscopic and differential interference images of GFP-expressing H460 cells treated with ZnPc-loaded liposomes followed by laser irradiation for (a) 1 and (b) 3 min. The cells were treated with ZnPc-loaded liposomes for 30 min, washed and irradiated with a 660 nm laser for 1 or 3 min. After irradiation, the cellular morphology was immediately visualized using confocal fluorescence microscopy. Control indicates the sample irradiated alone. Scale bar indicates 2 μm .

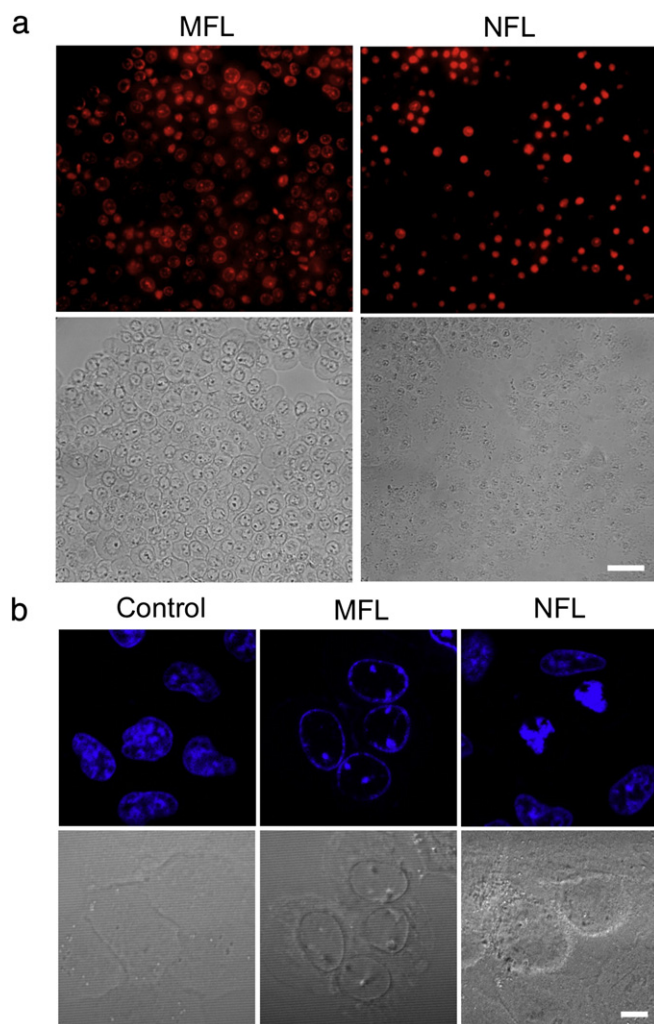


Fig. 6. Nuclear morphological changes in the H460 cells in the early stages after photodynamic therapy. (a) Epifluorescence microscopic and differential interference images of H460 cells stained with ethidium homodimer-1 (red) immediately after photodynamic therapy. Scale bar indicates 10 μm . (b) Confocal microscopic and differential interference images of H460 cells stained with Hoechst 33342 (blue) immediately after photodynamic therapy. The cells were treated with ZnPc-loaded liposomes for 30 min, washed and irradiated with a 660 nm laser. After irradiation, the cells were immediately stained with ethidium homodimer-1 or Hoechst 33342 and then imaged using a fluorescence or confocal fluorescence microscope. Control indicates the sample irradiated alone. Scale bar indicates 2 μm .

was observed primarily near the regions where the ZnPc molecules were initially delivered (plasma membrane for MFL-treated cells and intracellular compartments for NFL-treated cells), indicating that the PSs delivered selectively to the subcellular regions indeed contributed to the site-specific ROS generation. The amount of intracellular ROS generated in the cells treated with MFLs was not significantly different from that treated with NFLs (Fig. 7b). Taken together, these results suggest that the local ROS generation by ZnPc molecules embedded in the plasma membrane would be one of main contributors to the substantial membrane disruption. The effective cell death could be also partially caused by the local heat generated by membrane-localized ZnPc molecules upon irradiation [32,41].

4. Conclusions

In summary, we demonstrate that the selective delivery of hydrophobic PSs into the plasma membrane can significantly enhance the therapeutic efficacy of PDT. The MFLs designed to fuse with the plasma

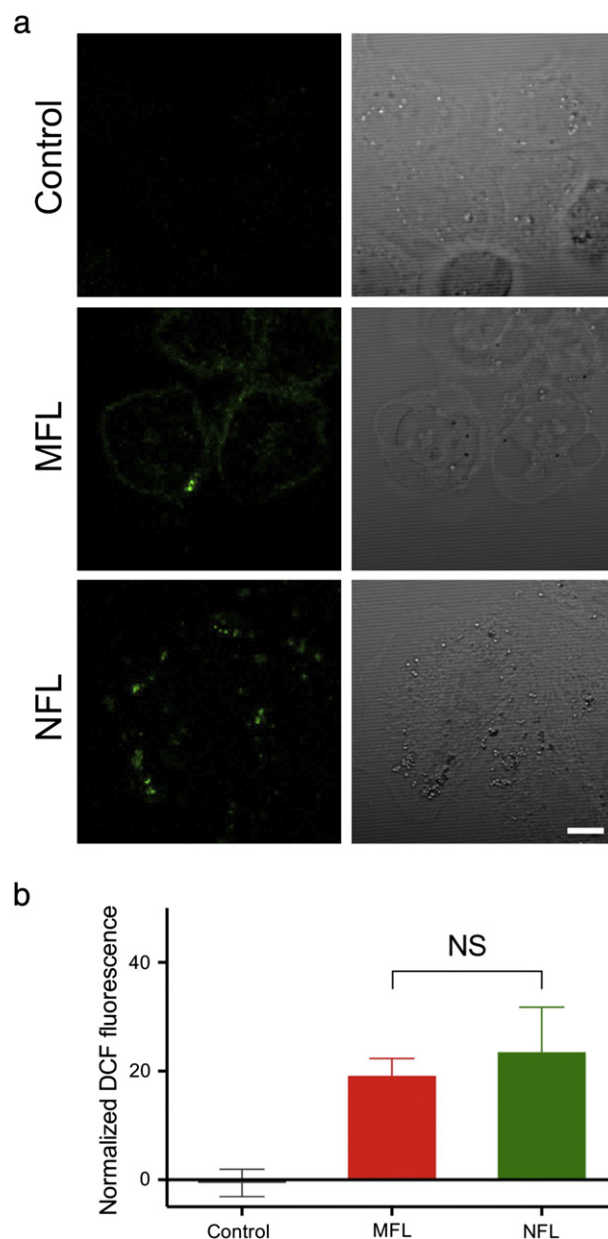


Fig. 7. Intracellular ROS generation in H460 cells in the early stages after photodynamic therapy. (a) Confocal fluorescence microscopic and differential interference images of DCFH-DA-loaded H460 cells immediately after photodynamic therapy. (b) Quantification of DCF fluorescence in the cells immediately after photodynamic therapy. The cells preloaded with DCFH-DA were treated with ZnPc-loaded liposomes for 30 min, washed, and irradiated with a 660 nm laser. For cellular imaging, the cells were imaged using a confocal fluorescence microscope immediately after irradiation. For fluorescence measurements, the cells were lysed with RIFA buffer after 30 min incubation, and the DCF fluorescence of the cell lysate was measured using a spectrofluorometer and normalized to the untreated sample ($n = 4$; error bars = s.d.; NS, not significant by one-way ANOVA). Control indicates the sample irradiated alone. Scale bar indicates 2 μm .

membrane were used to deliver the ZnPc molecules selectively into the plasma membrane. The phototoxicity of cells treated with ZnPc-loaded MFLs was significantly higher than that of cells treated with ZnPc-loaded NFLs, which is the conventional liposomal formulation that delivers the payload into the cytoplasm *via* endocytosis. The ZnPc molecules localized in the plasma membrane induced substantial membrane disruption upon irradiation, thereby leading to acute necrosis-like cell death. The local ROS generation by ZnPc molecules embedded in the plasma membrane primarily accounts for the effective disruption of plasma membrane. Looking further, the MFLs could be engineered to

deliver large amounts of hydrophobic PSs specifically into the tumor cell membranes *in vivo* by increasing their blood residence time and equipping them with tumor-targeting ligands. Such membrane-specific delivery may also amplify the retention of PSs in the tumor cells *in vivo*, enhancing PDT outcomes. Thus, the liposomal formulation that delivers the hydrophobic PSs selectively into the plasma membrane of target cells is a promising delivery system for the effective PDT of cancer.

Acknowledgements

This work was supported by the Basic Science Research Program (Grant No. NRF-2012R1A1A1011058) and the Global Frontier Project (Grant No. NRF-2013M3A6A4072541) through the National Research Foundation funded by the Ministry of Science, ICT & Future Planning, Republic of Korea. O.A.S. was supported by Conselho Nacional de Desenvolvimento Científico e Tecnológico (CNPq), Brazil.

Appendix A. Supplementary data

Supplementary data to this article can be found online at <http://dx.doi.org/10.1016/j.jconrel.2014.05.049>.

References

- [1] A. Urruticoechea, R. Alemany, J. Balart, A. Villanueva, F. Vinals, G. Capella, Recent advances in cancer therapy: an overview, *Curr. Pharm. Des.* 16 (2010) 3–10.
- [2] S.B. Brown, E.A. Brown, I. Walker, The present and future role of photodynamic therapy in cancer treatment, *Lancet Oncol.* 5 (2004) 497–508.
- [3] T.J. Dougherty, C.J. Gomer, G. Jori, D. Kessel, M. Korbelik, J. Moan, et al., Photodynamic therapy, *J. Natl. Cancer Inst.* 90 (1998) 889–905.
- [4] P. Agostinis, K. Berg, K.A. Cengel, T.H. Foster, A.W. Girotti, S.O. Gollnick, et al., Photodynamic therapy of cancer: an update, *CA Cancer J. Clin.* 61 (2011) 250–281.
- [5] Z. Huang, A review of progress in clinical photodynamic therapy, *Technol. Cancer Res. Treat.* 4 (2005) 283.
- [6] L.E. Rhodes, M. de Rie, Y. Enström, et al., Photodynamic therapy using topical methyl aminolevulinic acid vs surgery for nodular basal cell carcinoma: results of a multicenter randomized prospective trial, *Arch. Dermatol.* 140 (2004) 17–23.
- [7] D.E. Dolmans, D. Fukumura, R.K. Jain, Photodynamic therapy for cancer, *Nat. Rev. Cancer* 3 (2003) 380–387.
- [8] D. Kessel, Subcellular localization of photosensitizing agents: introduction, *Photochem. Photobiol.* 65 (1997) 387–388.
- [9] A.P. Castano, T.N. Demidova, M.R. Hamblin, Mechanisms in photodynamic therapy: part one—photosensitizers, photochemistry and cellular localization, *Photodiagn. Photodyn. Ther.* 1 (2004) 279–293.
- [10] C. Fabris, G. Valduga, G. Miotto, L. Borsetto, G. Jori, S. Garbisa, et al., Photosensitization with zinc (II) phthalocyanine as a switch in the decision between apoptosis and necrosis, *Cancer Res.* 61 (2001) 7495–7500.
- [11] Z. Malik, I. Amit, C. Rothmann, Subcellular localization of sulfonated tetraphenyl porphyrins in colon carcinoma cells by spectrally resolved imaging, *Photochem. Photobiol.* 65 (1997) 389–396.
- [12] C. Yow, J. Chen, N. Mak, N. Cheung, A. Leung, Cellular uptake, subcellular localization and photodamaging effect of temoporfin (mTHPC) in nasopharyngeal carcinoma cells: comparison with hematoporphyrin derivative, *Cancer Lett.* 157 (2000) 123–131.
- [13] A.A. Rosenkranz, D.A. Jans, A.S. Sobolev, Targeted intracellular delivery of photosensitizers to enhance photodynamic efficiency, *Immunol. Cell Biol.* 78 (2000) 452–464.
- [14] A.A. Rosenkranz, V.G. Lunin, O.V. Sergienko, D.G. Gilyazova, O.L. Voronina, D.E. Jans, et al., Targeted intracellular site-specific drug delivery: photosensitizer targeting to melanoma cell nuclei, *Russ. J. Genet.* 39 (2003) 198–206.
- [15] Y.N. Konan, J. Chevallier, R. Gurny, E. Allémann, Encapsulation of p-THPP into nanoparticles: cellular uptake, subcellular localization and effect of serum on photodynamic activity, *Photochem. Photobiol.* 77 (2003) 638–644.
- [16] D.K. Chatterjee, L.S. Fong, Y. Zhang, Nanoparticles in photodynamic therapy: an emerging paradigm, *Adv. Drug Deliv. Rev.* 60 (2008) 1627–1637.
- [17] M. Zhang, T. Murakami, K. Ajima, K. Tsuchida, A.S.D. Sandanayaka, O. Ito, et al., Fabrication of ZnPc/protein nanohorns for double photodynamic and hyperthermic cancer phototherapy, *Proc. Natl. Acad. Sci.* 105 (2008) 14773–14778.
- [18] R. Allison, H. Mota, V. Bagnato, C. Sibata, Bio-nanotechnology and photodynamic therapy—state of the art review, *Photodiagn. Photodyn. Ther.* 5 (2008) 19–28.
- [19] M. Fadel, K. Kassab, D.A. Fadeel, Zinc phthalocyanine-loaded PLGA biodegradable nanoparticles for photodynamic therapy in tumor-bearing mice, *Lasers Med. Sci.* 25 (2010) 283–292.
- [20] T. Nann, Nanoparticles in photodynamic therapy, *Nano Biomed. Eng.* 3 (2011).
- [21] S.J. Lee, H. Koo, D.-E. Lee, S. Min, S. Lee, X. Chen, et al., Tumor-homing photosensitizer-conjugated glycol chitosan nanoparticles for synchronous photodynamic imaging and therapy based on cellular on/off system, *Biomaterials* 32 (2011) 4021–4029.
- [22] L. Li, Z. Luo, Z. Chen, J. Chen, S. Zhou, P. Xu, et al., Enhanced photodynamic efficacy of zinc phthalocyanine by conjugating to heptalysine, *Bioconjug. Chem.* 23 (2012) 2168–2172.
- [23] J. Lin, S. Wang, P. Huang, Z. Wang, S. Chen, G. Niu, et al., Photosensitizer-loaded gold vesicles with strong plasmonic coupling effect for imaging-guided photothermal/photodynamic therapy, *ACS Nano* 7 (2013) 5320–5329.
- [24] A.S.L. Derycke, P.A.M. de Witte, Liposomes for photodynamic therapy, *Adv. Drug Deliv. Rev.* 56 (2004) 17–30.
- [25] C.S. Jin, G. Zheng, Liposomal nanostructures for photosensitizer delivery, *Lasers Surg. Med.* 43 (2011) 734–748.
- [26] M.S. Muthu, S.-S. Feng, Theranostic liposomes for cancer diagnosis and treatment: current development and pre-clinical success, *Expert Opin. Drug Deliv.* 10 (2013) 151–155.
- [27] E. Reddi, C. Zhou, R. Biolo, E. Menegaldo, G. Jori, Liposome- or LDL-administered Zn (II)-phthalocyanine as a photodynamic agent for tumours. I. Pharmacokinetic properties and phototherapeutic efficiency, *Br. J. Cancer* 61 (1990) 407–411.
- [28] A.M. Garcia, E. Alarcon, M. Munoz, J.C. Scaiano, A.M. Edwards, E. Lissi, Photophysical behaviour and photodynamic activity of zinc phthalocyanines associated to liposomes, *Photochem. Photobiol. Sci.* 10 (2011) 507–514.
- [29] V.P. Torchilin, Recent advances with liposomes as pharmaceutical carriers, *Nat. Rev. Drug Discov.* 4 (2005) 145–160.
- [30] Y.-J. Hsieh, C.-C. Wu, C.-J. Chang, J.-S. Yu, Subcellular localization of Photofrin(r) determines the death phenotype of human epidermoid carcinoma A431 cells triggered by photodynamic therapy: when plasma membranes are the main targets, *J. Cell. Physiol.* 194 (2003) 363–375.
- [31] N. Cauchon, M. Nader, G. Bkaily, J.E. Lier, D. Hunting, Photodynamic activity of substituted zinc trisulfophthalocyanines: role of plasma membrane damage, *Photochem. Photobiol.* 82 (2006) 1712–1720.
- [32] M. Mitsunaga, M. Ogawa, N. Kosaka, L.T. Rosenblum, P.L. Choyke, H. Kobayashi, Cancer cell-selective *in vivo* near infrared photoimmunotherapy targeting specific membrane molecules, *Nat. Med.* 17 (2011) 1685–1691.
- [33] M.E. Bulina, D.M. Chudakov, O.V. Britanova, Y.G. Yanushevich, D.B. Staroverov, T.V. Chepurnykh, et al., A genetically encoded photosensitizer, *Nat. Biotechnol.* 24 (2006) 95–99.
- [34] M.N. Sibata, A.C. Tedesco, J.M. Marchetti, Photophysical and photochemical studies of zinc(II) phthalocyanine in long time circulation micelles for photodynamic therapy use, *Eur. J. Pharm. Sci.* 23 (2004) 131–138.
- [35] G. Gopalakrishnan, C. Danelon, P. Izewska, M. Prummer, P.-Y. Bolinger, I. Geissbühler, et al., Multifunctional lipid/quantum dot hybrid nanocontainers for controlled targeting of live cells, *Angew. Chem. Int. Ed.* 45 (2006) 5478–5483.
- [36] S. Krasnici, A. Werner, M.E. Eichhorn, M. Schmitt-Sody, S.A. Pahernik, B. Sauer, et al., Effect of the surface charge of liposomes on their uptake by angiogenic tumor vessels, *Int. J. Cancer* 105 (2003) 561–567.
- [37] C.R. Miller, B. Bondurant, S.D. McLean, K.A. McGovern, D.F. O'Brien, Liposome-cell interactions *in vitro*: effect of liposome surface charge on the binding and endocytosis of conventional and sterically stabilized liposomes, *Biochemistry* 37 (1998) 12875–12883.
- [38] R.R. Perry, W. Matthews, J.B. Mitchell, A. Russo, S. Evans, H.I. Pass, Sensitivity of different human lung cancer histologies to photodynamic therapy, *Cancer Res.* 50 (1990) 4272–4276.
- [39] V.L. Johnson, S.C. Ko, T.H. Holmstrom, J.E. Eriksson, S.C. Chow, Effector caspases are dispensable for the early nuclear morphological changes during chemical-induced apoptosis, *J. Cell Sci.* 113 (2000) 2941–2953.
- [40] S.A. Susin, E. Daugas, L. Ravagnan, K. Samejima, N. Zamzami, M. Loeffler, et al., Two distinct pathways leading to nuclear apoptosis, *J. Exp. Med.* 192 (2000) 571–580.
- [41] W.P. Thorpe, M. Toner, R.M. Ezzell, R.G. Tompkins, M.L. Yarmush, Dynamics of photoinduced cell plasma membrane injury, *Biophys. J.* 68 (1995) 2198–2206.